Available online at www.sciencedirect.com
ScienceDirect
European Journal of Pharmaceutics and Biopharmaceutics 64 (2006) 307–315
European Journal of Pharmaceutics and Biopharmaceutics
www.elsevier.com/locate/ejpb

Research paper

Dynamic moisture sorption and desorption of standard and silicified microcrystalline cellulose

K. Kachrimanis [a,*], M.F. Noisternig [b], U.J. Griesser [b], S. Malamataris [a]

[a] Department of Pharmaceutical Technology, School of Pharmacy, University of Thessaloniki, Thessaloniki, Greece
[b] Department of Pharmaceutical Technology, Institute of Pharmacy, University of Innsbruck, Innsbruck, Austria

Received 6 March 2006; accepted in revised form 31 May 2006
Available online 9 June 2006

Abstract

Moisture sorption and desorption isotherms of standard and silicified microcrystalline cellulose (MCC and SMCC) were determined using an automatic multi-sample gravimetric analyzer, and compared by fitting different kinetic models, including the excess surface work model (ESW), the BET and GAB model, Young and Nelson model and recently developed parallel exponential kinetics (PEK) model. It was found that silicification affects the moisture sorption and desorption properties of SMCC mainly at high relative humidity (above 50% and 70%, respectively). In general, the differences in the moisture sorption and desorption properties of MCC and SMCC can be elucidated by the different kinetic models. Particularly the PEK model shows that hysteresis is related primarily to a fast sorption process, which corresponds to bound water, and secondarily to a slow process, which corresponds to sorption of free water and that SMCC acquires more water than MCC at RH higher than 50% by the slow (secondary) sorption process. A possible mechanism for this process is presumably the hydrolysis of SiO_2 particles and formation of silanol groups that act as a water reservoir, preventing the accumulation of more water in the polymer matrix and thus may be protecting the structure of SMCC from undergoing irreversible structural changes that would impair its performance as an excipient.

Keywords: Moisture sorption; Isotherms; Microcrystalline cellulose; Silicified microcrystalline cellulose; Parallel exponential kinetics

1. Introduction

Microcrystalline cellulose (MCC) is by far the most widely used direct compression and wet granulation pharmaceutical excipient, but several limitations to its functionality have been pointed out, such as poor flow and packing, great dependence of disintegration on the compression load, excessive mechanical strength of tablets, high sensitivity on lubricant and moisture content, and deterioration of compression properties after wet granulation [1]. Most of the aforementioned formulation problems are related to the interactions of MCC with water. Specifically, the sensitivity of MCC to wet granulation is related to an abrupt increase in granule density upon drying, attributed to the formation of new H-bonds between hydroxyl groups previously occupied by water molecules, a process known as "hornification" in the wood-pulp industry [2]. Furthermore, it has been shown that even small batch-to-batch variations in residual water content can have a significant effect on MCC compression properties [3].

In an attempt to overcome the limitations in MCC functionality, a product known as silicified-MCC (SMCC) was marketed [4]. Comparative studies have failed to identify any bulk chemical change in the amorphous or crystalline regions of MCC due to the silicification process [5], or any difference in the enthalpy of water sorption [6], and the improved performance of the silicified-MCC was presumably attributed to the surface modification of the MCC particles. Particularly, the resistance of SMCC to the effects of wet granulation indicates differences in the mechanism of water sorption and desorption and further

* Corresponding author. Department of Pharmaceutical Technology, School of Pharmacy, University of Thessaloniki, 54124 Thessaloniki, Greece. Tel.: +302 31 0 997666; fax: +302 31 0 997652.
E-mail address: kgk@pharm.auth.gr (K. Kachrimanis).

0939-6411/$ - see front matter © 2006 Elsevier B.V. All rights reserved.
doi:10.1016/j.ejpb.2006.05.019

evidence for the existence of differences in the hydration process between standard and silicified MCC was the significantly higher disintegration time of SMCC compacts compared to that of corresponding MCC compacts after storage at different % RH environments [7]. It was found that at high relative humidity (72% RH) the incorporated SiO_2 reduces the energy of interparticle bonding and the interparticle separation, resulting in more extended disintegration times due to reduced uptake of water into the tablets and to the probable reduction of water available for the deployment of the microcrystalline cellulose activity as disintegrant.

The effects of moisture sorption on the solid state properties of excipients have been recently discussed [8], and particularly the interactions of various celluloses with water, and the relations with crystallinity, have been investigated [9]. Different methods have been utilized, and it has been established that water is sorbed almost exclusively by the amorphous regions of MCC. Moreover, gravimetric determination of dynamic moisture sorption followed by theoretical BET isotherm analyses [10,11] as well as experimental dielectric response measurements [12], suggested the attachment of a single water molecule per anhydroglucose unit, while differential scanning calorimetry (DSC) studies revealed a value of 3.4 non-freezing bound water molecules per anhydroglucose unit [13,14]. The fractional number could be resulting from the association of a water molecule with two adjacent anhydroglucose units, or from the dependence of water H-bonding patterns on the conformation of the cellobiose dimer [13]. However, until now the mechanism by which the presence of colloidal SiO_2 particles on the surface of silicified MCC affects its interactions with water is not fully understood. Therefore, in the present study, elucidation of the effects of silicification on the water sorption and desorption process is attempted by employing a sensitive automatic multi-sample gravimetric sorption analyzer and comparing for MCC and SMCC the fitting parameters and constants involved in different kinetic models. The kinetic models selected are those commonly applied for pharmaceutical materials and a newly developed parallel exponential kinetics (PEK) model [15]. The last assumes two parallel independent first order processes, a fast and a slow one, taking place simultaneously to describe moisture sorption and desorption by two different mechanisms related to sites with different accessibility and affinity to water molecules.

2. Materials and methods

2.1. Materials

Avicel® PH 101, NF/EP Lot: 6950C (FMC International, Little Island, Cork, Ireland), the first MCC product introduced in the market, and Prosolv® 50, Lot: P5S0010, (Penwest Pharmaceuticals Co., Nastola, Finland) were selected as standard and silicified-MCC, respectively. The <63 μm size fraction was separated by sieving and used, to minimize the effects of possible differences in the intraparticle porosity and therefore in moisture sorption and desorption. Crystallinity of both MCC and silicified-MCC was determined by employing PXRD analysis.

2.2. Methods

2.2.1. Dynamic moisture sorption and desorption

An automatic multi-sample moisture sorption analyzer SPS11 (Projekt-Messtechnik, D-Ulm) was used, equipped with a specially designed climatic chamber, an analytical balance with a resolution of 10 μg (AB135-S, Mettler Toledo Inc.) and a sample changer. The instrument allows a continuous monitoring of the mass changes of 11 samples, which are exposed to the same atmospheric conditions. The samples are sequentially weighed and the humidity is kept constant until all of the samples meet a preset equilibrium condition. Three samples of approximately 1.0 g of each excipient were pre-equilibrated over a saturated K_2CO_3 solution (43% RH) before they were uniformly spread in aluminum sample dishes of 5 cm diameter and placed in the moisture sorption analyzer. The measuring cycle was started at 43% relative humidity (RH %) followed by an equilibration step at 0% RH. Then the moisture sorption–desorption cycle was started at 25.0 ± 0.1 °C, increasing the relative humidity by 5% RH intervals. The variation of the humidity values was less than ±0.5% and the mass change of the samples was recorded every 8 min. The equilibrium condition was set to <0.01% total mass change within 40 min and when it was fulfilled the relative humidity was automatically increased by 5% RH until 95% RH and then decreased down to 0% RH following the same stepwise manner.

Gravimetric moisture sorption/desorption analysis provides only the relative mass change as function of RH. The mass change (in %) is usually calculated on the basis of the lowest mass at the driest condition (close to 0%). However, strongly bound water that cannot be removed at this condition may be still present in the polymer and in order to calculate the absolute water content of the sample as a function of RH the absolute water content of the sample at any RH must be determined. In this study, an appropriate correction was performed on the basis of the absolute moisture content determined by thermo-gravimetric analysis (TGA) on three extra samples stored over a saturated K_2CO_3 solution (43% RH, desiccator 25 °C). The level of 43% RH was chosen as storage condition before the measurement as well as starting and end condition of the moisture sorption experiment. This conditioning, close to the average atmospheric RH in the laboratory, guarantees uniform starting conditions for all samples and no or minor change in the water content during handling of the samples before or after the sorption/desorption measurements.

The automatic multi-sample analyzer is able to provide information only for the relative weight change of the sample. However, strongly bound water may be present

in the polymer matrix that cannot be removed by drying at 0% RH and 25 °C temperature in the analyzer (actual RH in climatic chamber, 0.2%). Such water was determined comparing data of the multi-sample moisture sorption analyzer and TGA determination of moisture content.

2.2.2. TGA determination of the water content

About 5 mg of material was subjected to isothermal TGA, at 105 °C for 180 min, using a Perkin-Elmer TGA-7 system (Perkin-Elmer, Norwalk, CT, USA) interfaced to a computer running the Pyris 2.0 software. The experiments were repeated in triplicate. TGA was applied because it resulted in better reproducible absolute water content values than Karl–Fischer titration.

2.2.3. PXRD analysis and determination of crystallinity

The powder X-ray diffraction (PXRD) experiments were conducted using a Siemens D-5000 diffractometer (Siemens AG, Karlsruhe, Germany) equipped with a theta/theta goniometer, a CuK_α radiation source, a Goebel mirror (Bruker AXS, Karlsruhe, Germany), a 0.15° soller slit collimator and a scintillation counter. The patterns were recorded at a tube voltage of 40 kV and a current of 35 mA, at a scan rate of 0.005° 2θ/s in the angular range of 2–40° 2θ. The crystallinity index (CI) was calculated by the peak intensity method [16] using the formula:

$$\mathrm{CI} = \frac{I_{200} - I_{\mathrm{am}}}{I_{200}} \tag{1}$$

where I_{200} is the intensity of the 200 reflection at 22.6° 2θ, and I_{am} is the baseline intensity at 18.7° 2θ.

2.2.4. Isotherms comparison and model fitting

2.2.4.1. Analysis of hysteresis. Sorption/desorption hysteresis may provide information about structural changes due to the interaction with water and was quantified at each equilibration step using both the adsorption–desorption ratio [10] and the degree of hysteresis [17], according to the equation:

$$\text{Degree of hysteresis}(\%) = 100 \times \left(\frac{M_{\mathrm{des}} - M_{\mathrm{sor}}}{M_{\mathrm{sor}}}\right) \tag{2}$$

where M_{des} is the equilibrium water content during desorption and M_{sor} is the corresponding equilibrium water content during the sorption phase (%w/w).

2.2.4.2. Excess surface work (ESW) model. According to Adolphs and Setzer [18–20], ESW is defined the product of the adsorbed amount and the change in chemical potential, which is then plotted versus the adsorbed amount. The ESW yields a minimum that coincides with the monolayer capacity. The ESW can be calculated from the equation:

$$\Phi = w_{\mathrm{ads}}\Delta\mu = w_{\mathrm{ads}}RT\ln(a_w) \tag{3}$$

where Φ is the ESW, w_{ads} is the number of sorbed molecules, $\Delta\mu$ is the change in the chemical potential, R is the gas constant, T is the absolute temperature and a_w is the water activity (equal to RH for temperature up to 50 °C). The linearized form of the ESW model was used in the present study for the calculation of the onset potential $\Delta\mu_o$ or driving force for the water sorption and monolayer water w_{m}, as described by Adolphs and Setzer from plots of $\ln|\Delta\mu|$ versus w_{ads} [20]:

$$\ln|\Delta\mu| = -\tfrac{1}{w_{\mathrm{m}}}w_{\mathrm{ads}} + \ln|\Delta\mu_0| \tag{4}$$

where w_{m} is the amount of monolayer water, and $\Delta\mu_o$ is the onset potential. $\Delta\mu$ equals the product $RT\ln(a_w)$ and for powdered materials, where capillary condensation may occur, the ESW model yields a second minimum in the $\ln|\Delta\mu|$ versus w_{ads} curve, which consists of two linear parts with different slopes that can be estimated by fitting a different linear regression in each linear part.

2.2.4.3. BET and GAB model. The original and the extended Brunauer–Emet–Teller (BET) equation according to the modifications of Guggenheim, Anderson and de Boer, known as the GAB equation [21], was fitted to the moisture sorption isotherms:

$$w = \frac{\{ckw_{\mathrm{m}}a_w\}}{(1-ka_w)(1-ka_w+cka_w)} \tag{5}$$

where w is the weight of sorbed water per gram of solid, w_{m} is the weight of water in the form of a monolayer, a_w is the water activity, and c and k are parameters related to the enthalpy of sorption, given by the equations:

$$k = B_1\exp\left[\frac{H_{\mathrm{L}} - H_{\mathrm{m}}}{RT}\right] \tag{6}$$

$$c = D\left[\frac{H_1 - H_{\mathrm{m}}}{RT}\right] \tag{7}$$

where B_1 and D are constants, H_{L} is the heat of condensation of water, H_1 is the heat of sorption of water sorbed in the monolayer, H_{m} is the heat of sorption of water in multilayers built up on that monolayer, R is the ideal gas constant, and T is the absolute temperature. When $k = 1$, Eq. (2) corresponds to the BET model, and is applicable to the relative humidity range from 0 to ~40%. The GAB model has more general applicability over a wider water activity range, and its parameters are considered to be more accurate [22].

2.2.4.4. Young and Nelson model. The Young and Nelson equations [23,24], which distinguish between tightly bound monolayer, normally condensed externally adsorbed moisture and internally absorbed water, were also fitted to the sorption–desorption isotherms by a combination of multiple regression and nonlinear iteration procedure [25]:

$$\theta = \frac{\mathrm{RH}}{\mathrm{RH} + (1-\mathrm{RH})E} \tag{8}$$

$$\psi = \mathrm{RH}\theta \tag{9}$$

$$\beta = -\frac{E\mathrm{RH}}{E-(E-1)\mathrm{RH}} + \frac{E^2}{E-1}\ln\frac{E-(E-1)\mathrm{RH}}{E} - (E+1)\ln(1-\mathrm{RH}) \tag{10}$$

$$M_s = A(\theta + \beta) + B\psi \quad (11)$$

$$M_d = A(\theta + \beta) + B\theta RH_{max} \quad (12)$$

where θ is the fraction of surface covered by a monomolecular layer, ψ is the fraction of surface covered by a layer of water two or more molecules thick, β is the total amount of adsorbed moisture in a multilayer, M_s and M_d are the moisture contents during sorption and desorption, respectively, and RH and RH_{max} are the relative humidity and the maximum relative humidity, respectively. A, B, and E are parameters characteristic of the material, given by the relations:

$$E = \exp[-(q_1 - q_L)kT] \quad (13)$$

$$A = \frac{\rho_w V_m}{W'_m} \quad (14)$$

$$B = \frac{\rho_w V_a}{W'_m} \quad (15)$$

where, q_1 is the heat of adsorption of water bound to the surface, q_L is the heat of normal condensation, k is the Boltzmann constant, and T the temperature, V_m and V_a are the volumes of the adsorbed and absorbed moisture, respectively, ρ_w is the density of water and W'_m is the mass of dry material. The product $A\theta$ gives the amount of monolayer moisture, $A(\theta + \beta)$ is the externally adsorbed moisture and $B\psi$ is the amount of absorbed moisture during the sorption phase. The goodness of fit was evaluated on the basis of the average percent deviation [26] and the correlation coefficient, calculated as follows:

$$R = \sqrt{1 - \frac{ESS}{EMS}} \quad (16)$$

where ESS is the sum of squares of the deviation of the observed from the predicted by the model values, and EMS is the sum of squares of the deviation of the observed values from their mean [25].

2.2.4.5. Parallel exponential kinetics (PEK) model. The PEK model [15] is an empirical one whose applicability has been demonstrated in different cellulosic textile materials [17]. Besides an excellent fit to the experimental data, it provides a set of easily interpretable, physically meaningful parameters. It assumes two parallel independent first order processes taking place simultaneously to describe vapor sorption and desorption by two different mechanisms or components (fast and slow) related to sites with different accessibility and affinity to water molecules. Particularly, it provides insight into the time scales (rates) and the mass changes (extents) of the individual components. Experimental moisture content is simulated as a function of time separately at each equilibration step using Eqs. (17) and (18):

$$M_t = M_{\infty 1}\left(1 - e^{-t/\tau_1}\right) + M_{\infty 2}\left(1 - e^{-t/\tau_2}\right) \quad (17)$$

$$M_\tau = M_\infty\left(1 - e^{-1}\right) \approx 0.6321 M_\infty \quad (18)$$

where M_t and M_∞ are the mass change at time t and at equilibrium state, and τ is a characteristic time to obtain approximately 63% of M_∞. Subscripts 1 and 2 indicate a fast and a slow kinetic process, corresponding to sites with high and low affinity with water, respectively. The fast and slow water affinity sites are presumably related to different types of amorphous regions, external or internal surfaces, voids or crystallites, and direct binding of water on hydroxyl groups or indirect binding on top of directly bound water [27]. Direct sorption onto the external surfaces and amorphous regions should be fast, while indirect sorption should be slower, since it is energetically less favorable. PEK parameters $M_{\infty 1}$ and $M_{\infty 2}$ were calculated for each equilibration step.

The JMP-IN v. 5.1 (SAS Institute Inc.) nonlinear regression routine was used for model fitting and evaluation of the goodness of fit. Particularly for the Young and Nelson model, a combination of nonlinear iteration and multiple regression was used, as described in [24,25]. An arbitrarily chosen value of E was used to calculate θ, ψ, and β, and those values were substituted into Eqs. (11) and (12) in order to obtain theoretical values of M_s and M_d at various RH levels. Subsequently, the correlation coefficient, R, between experimental and theoretical moisture content was calculated by Eq. (16). This process was repeated until the value of E maximizing R and minimizing the percent deviation between theoretical and experimental moisture contents was found, and the corresponding A and B values were calculated by multiple linear regression using Eqs. (11) and (12), with the help of an MS Excel spreadsheet.

3. Results and discussion

3.1. Moisture sorption and desorption isotherms

The water content determined by isothermal TGA for samples equilibrated at 43% RH was found to be similar for both polymers (5.3% for MCC and 5.2% for SMCC), but larger than that obtained by using the automatic multi-sample moisture sorption analyzer (4.4% for MCC and 4.3% for SMCC). This indicates that the dry starting material contains a ~1% amount of strongly bound water that cannot be removed by equilibration at the driest condition in the climatic chamber of the multi-sample analyzer. Therefore, the relative mass changes obtained from the moisture sorption analysis were corrected taking into account the water content determined by TGA (43% RH), in order to reflect the absolute moisture content. Furthermore, the similarity between MCC and SMCC in the amount of this strongly bound water at about 0% RH is an indication that the SiO_2 particles on the surface of SMCC do not contribute in any relatively strong interaction with water, otherwise this amount would be remarkably different for SMCC.

In Fig. 1(a) plots of the percent mass change and the recorded relative humidity vs time are presented for the whole sorption–desorption cycle, and in Fig. 1(b) the

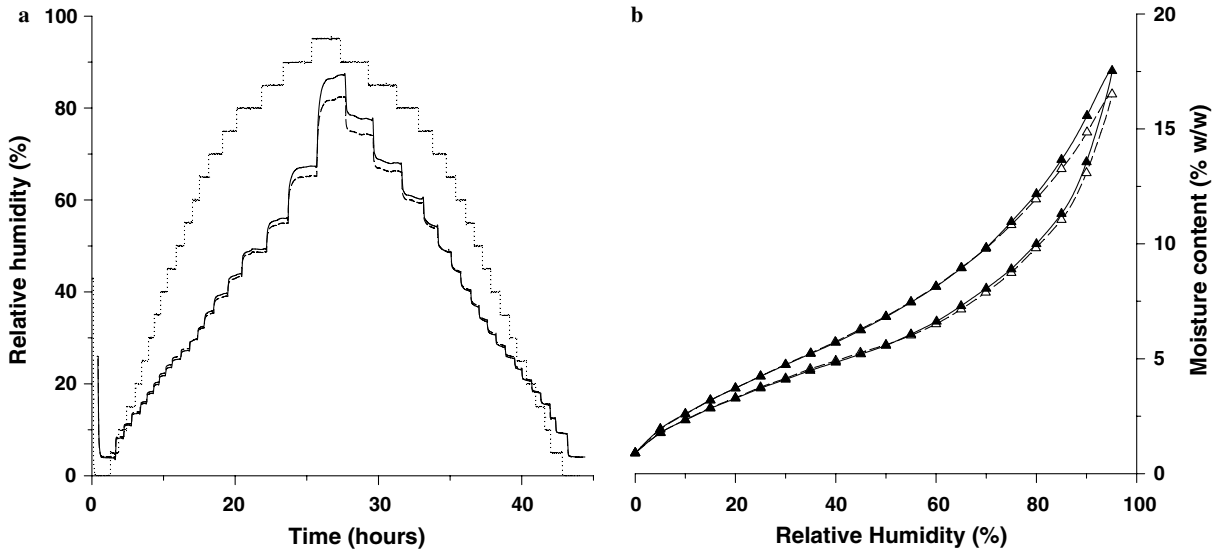

Fig. 1. (a) Plots of percent (%w/w) mass change (SMCC: solid line, MCC: dashed line) and percent relative humidity (dotted line) versus time, and (b) sorption and desorption isotherms of SMCC (full symbols), and MCC (empty symbols) after correction for the absolute water content determined by TGA ($n = 3$, SD < 0.1).

corrected sorption/desorption isotherms of MCC and SMCC are shown. For both MCC and SMCC the sorption isotherms have a characteristic type II shape, exhibiting a significant upswing at RH higher than 80%, which may originate from the water liquefaction due to capillary condensation into pores [28]. Furthermore, the shapes and positions of the isotherms are almost identical up to 50% RH, but above this limit, the sorption branch of SMCC starts to deviate progressively, as SMCC takes up more water than MCC. As far as the desorption branches are concerned they show similarity for a wider RH range (below 70%).

The difference between MCC and SMCC in the sorption process could be attributed to the presence of extra adsorption sites in the surface of SMCC, due to the silicification process (treatment with colloidal SiO_2 particles). However, these adsorption sites do not participate in the sorption process at RH lower than 50%, but they seem to be gradually "activated" above that limit. This can be explained by the fact that water molecules require fairly high amounts of energy to diffuse into amorphous silica, particularly through pentamer and hexamer rings. The energy barrier may be even higher when Si atoms are bridged together through oxygen atoms in a polymer network, as is the case of colloidal silicon dioxide, and can reach 140 kJ/mol of hydroxyl group formed [29]. The lowest energy interaction of water with SiO_2 is the formation of geminal and single silanol groups [30]. This means that, while at the lower relative humidity range very little or no water is adsorbed on – or absorbed into – the SiO_2 particles, at higher relative humidity, SiO_2 can react with water to form silanol groups that act as extra adsorption sites. Therefore, the SiO_2 particles keep taking up water after all high affinity sites of cellulose have been occupied, and this is reflected in the higher water content that SMCC acquires at the high relative humidity range. Thus, it is reasonable to assume that SiO_2 particles act as water reservoir at high RH environments, preventing the arrival of water in the polymer matrix and protecting the structure of SMCC from undergoing irreversible changes that would impair its performance.

3.2. Hysteresis

Data of hysteresis expressed either as sorption/desorption ratio or degree of hysteresis, in Table 1, follow similar pattern of gradual decrease or increase to a minimum or

Table 1
Hysteresis data expressed as sorption/desorption ratio and as degree of hysteresis

Relative humidity (%)	Sorption/desorption ratio		Degree of hysteresis (%)	
	MCC	SMCC	MCC	SMCC
5	0.86	0.83	15.8	20.6
10	0.86	0.84	16.7	19.3
15	0.86	0.84	16.6	18.5
20	0.85	0.84	17.5	18.8
25	0.86	0.85	16.8	18.3
30	0.84	0.83	18.4	19.8
35	0.84	0.83	18.7	20.5
40	0.83	0.82	20.6	21.9
45	0.81	0.80	23.3	24.3
50	0.79	0.79	26.4	26.6
55	0.78	0.79	28.5	26.9
60	0.77	0.79	29.3	26.4
65	0.78	0.79	28.8	25.8
70	0.79	0.80	27.3	24.7
75	0.79	0.80	26.6	25.6
80	0.81	0.81	23.9	23.9
85	0.82	0.82	21.8	22.6
90	0.87	0.86	14.5	15.9

maximum, respectively, at 60% RH for MCC and 50–65 or 55% RH for SMCC. There are characteristic differences between the two polymers, not only in the position of maximum hysteresis, but also in the magnitude. SMCC shows larger hysteresis than MCC at RH levels lower than 50%, while within the range of 55–75% RH, the order is reversed. At RH above 75%, very small difference in the degree of hysteresis is found.

Hysteresis at high relative humidities, typically higher than 75%, is usually attributed to pore-effects (''ink bottle'' pores), while that at lower relative humidity, to swelling due to specific interactions of water sorbed in the bulk, and according to novel approaches hysteresis is considered as the result of adsorption metastability rather than of desorption [31,32]. The lower hysteresis of SMCC in the RH range of 55–75% may be an indication of weaker specific interactions of its hydrophilic sites with water, and consequently, smaller structural changes due to polymer swelling. Therefore, the operation of silanol groups as additional adsorption sites at high RH range that is evident from the isotherms, Fig. 1(b), seems to offer some ''protection'' against irreversible structural reorganization of the MCC chains (''hornification''), as reflected by the lower hysteresis.

3.3. Kinetic model fitting

In Table 2 the fitting parameters and constants for the BET, GAB, Young and Nelson, and PEK model are listed. From the corresponding correlation coefficients (R^2, R, and R^2_{adj}) it can be seen that all models (Except the Young and Nelson model) fit the experimental data reasonably well. Regarding the Young and Nelson model, the percent deviation values, Table 2, show a hardly acceptable fit, as the limit is considered to be the value of 5% [26].

The ESW model predicts equal monolayer water values, w_m for both polymers, unlike BET monolayer parameters. The ESW model presumes the existence of two energetically distinct sorption processes, one equivalent with BET monolayer adsorption, that could reflect the association of water with high affinity adsorption sites (e.g., anhydroglucose hydroxyl groups) and a second process that could be interpreted as the sorption of water molecules after all high affinity sites have been occupied, e.g., in pores or by natural condensation. However, for the second sorption process, which takes place at the higher RH range, the ESW model predicts correctly a slightly higher water amount for SMCC, in agreement with the experimental findings.

The BET model predicts lower monolayer water values (w_m) than the GAB model and higher energy parameters (c), which is in agreement with Timmermann [22]. The energy parameters of both BET and GAB models are slightly higher for MCC than for SMCC, indicating that the driving force for water sorption is higher. The w_m parameters indicate that MCC acquires a slightly lower amount of water according to the BET model but a slightly higher according to the GAB model than SMCC in the presumed state of a monomolecular layer (water associated with high affinity adsorption sites).

Table 2
Fitting coefficients and parameters for different kinetic models

Model	Parameters	MCC	SMCC
$ESW_{1st\ process}$	R^2	0.999	0.999
	$\Delta\mu_{o1}$ (kJ/mol)	829.5	825.1
	w_m (% w/w)	2.70	2.69
$ESW_{2nd\ process}$	R^2	0.998	0.999
	$\Delta\mu_{o2}$ (kJ/mol)	324.7	337.5
	w_2 (% w/w)	4.31	4.68
BET	R^2	0.996	0.997
	c	10.35	10.05
	w_m (%w/w)	2.08	2.63
GAB	R^2	0.995	0.995
	c	8.16	8.00
	k	0.82	0.84
	w_m (% w/w)	3.26	3.21
Young & Nelson	R	0.986	0.988
	E	0.187	0.215
	A	0.032	0.034
	B	0.012	0.012
	% Deviation		
	Sorption	6.0	8.4
	Desorption	6.4	5.0
PEK model	Sorption		
	R^2_{adj}	0.999 ± 0.0007	0.999 ± 0.0008
	SE	0.0056 ± 0.0067	0.0041 ± 0.0029
	Mean $\lvert\Delta m\rvert$	0.0148 ± 0.0321	0.0118 ± 0.0136
	Desorption		
	R^2_{adj}	0.997 ± 0.005	0.996 ± 0.008
	SE	0.0054 ± 0.0034	0.0072 ± 0.0079
	Mean $\lvert\Delta m\rvert$	0.0051 ± 0.0158	0.0057 ± 0.0115

Coefficient of determination (R^2), monolayer water capacity (w_m), and energy parameters (c, k, and $\Delta\mu_o$), for the BET, GAB, and ESW models. Material characteristic parameters (E, A, and B) and average % deviation, for the Young and Nelson model.
Adjusted coefficient of determination ($R^2_{adj} = R^2 - (1 - R^2) * [(k - 1)/(n - k)]$, accounting for the different number of observations, n, obtained at different RH levels; k is the number of parameters), standard error of fit (SE), and difference between experimental and calculated by the model amount of sorbed water ($|\Delta m|$), for the PEK model (mean ± SD).

Considering the energy parameters of the ESW model, the driving force for water sorption ($\Delta\mu_{o1}$) is slightly higher for MCC, in agreement with the values of the BET–GAB models, and the assumed less tight binding of silanol with water may facilitate the mobility of water which results in lower $\Delta\mu_{o1}$ for SMCC. Furthermore, for the second sorption process of both SMCC and MCC, $\Delta\mu_{o2}$ is about one-third in magnitude compared to that of the first sorption process. This supports the view that the second process can be interpreted as indirect sorption of water by an energetically less demanding mechanism.

The estimated monolayer, externally, and internally absorbed moisture component isotherms according to the Young and Nelson model, Fig. 2, show that adsorption of a monolayer water is almost complete at about 50% RH for both polymers, having a type I shape (Langmuir

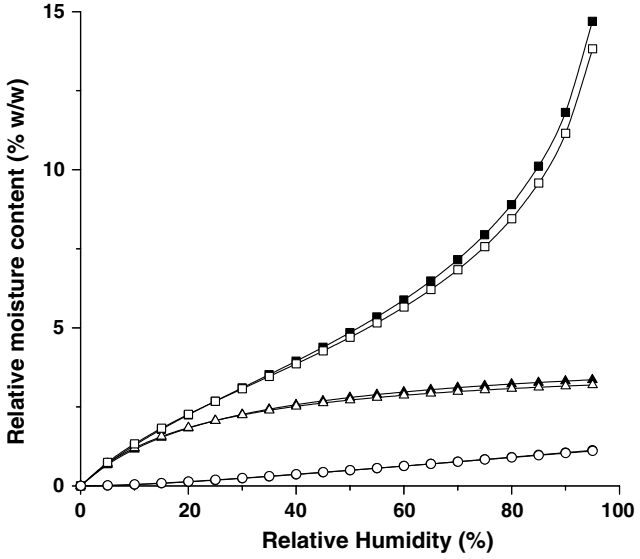

Fig. 2. Monolayer (▲), externally adsorbed (■), and internal (●) moisture component isotherms of SMCC (full symbols) and MCC (empty symbols), according to the Young and Nelson model.

isotherm), while the external moisture component isotherm has a type II shape and its contribution to the total amount of sorbed moisture increases with increasing RH. Finally, the ''internal'' moisture component increases linearly with the environmental relative humidity, but its overall contribution is generally small. Regarding the monolayer water, only negligible differences between MCC and SMCC are predicted, while the amount of ''internal'' moisture is equal for MCC and SMCC. But the most striking difference lies in the predicted amounts of ''external'' moisture, where SMCC shows clearly a higher capacity, with the difference increasing with the RH level. This is a clear indication of water sorption on silanol groups, which obviously is not behaving like monolayer because it is less tightly bound.

Regarding the characteristic times (dotted lines in Fig. 3) for the components (fast and slow) of the sorption and desorption process, which are inversely related to the process rate, their plots vs the RH show that: (a) The rate of fast sorption (full symbols) decreases at high RH (85–95%), while the rate of fast desorption (full symbols) remains constant (very high) up to 90% RH. (b) The rate of slow sorption (empty symbols) increases very slightly as RH is increased at low RH (0–10%) but only for MCC, while at high RH (80–95%) it decreases remarkably. (c) The rate of slow desorption (empty symbols) decreases remarkably as RH is increased at low RH (0–10%) but remains constant (relatively low) for all the other regions of RH, as expected.

The absence of a remarkable change in the rate of both fast and slow sorption up to 80% RH and the subsequent decrease is in agreement with the finding that for MCC the enthalpy of sorption is constant (-58 ± 5 kJ/mol) up to 80% RH, but above 80% it is decreased to 44 ± 5 kJ/mol (liquefaction enthalpy), as more freezing (normal or free) water starts to be absorbed [13]. Therefore, it is reasonable to interpret the ''fast'' sorption process mainly as the sorption of both types of bound water (non-freezing and freezing).

Regarding data of the mass change parameter in PEK model (solid lines in Fig. 3), it is seen that more water is both sorbed and desorbed by the fast sorption process (full symbols) at all RH levels, except the region above 70% RH regarding the sorption process for SMCC, as well as the region 75–85% regarding the sorption process of MCC.

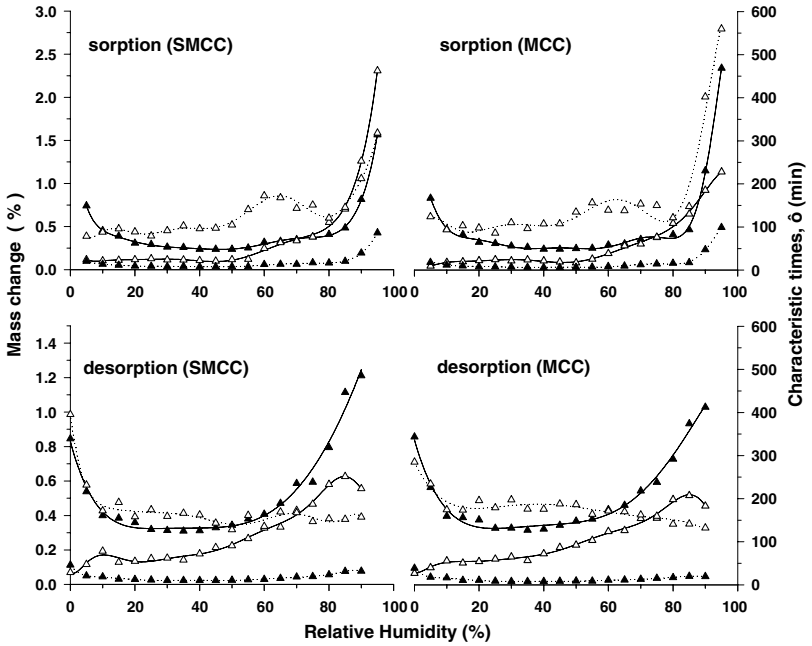

Fig. 3. Characteristic times (dotted lines) and mass parameters (solid lines) for the fast (full symbols) and slow (empty symbols) component of sorption and desorption process, derived on the basis of PEK model for MCC and SMCC.

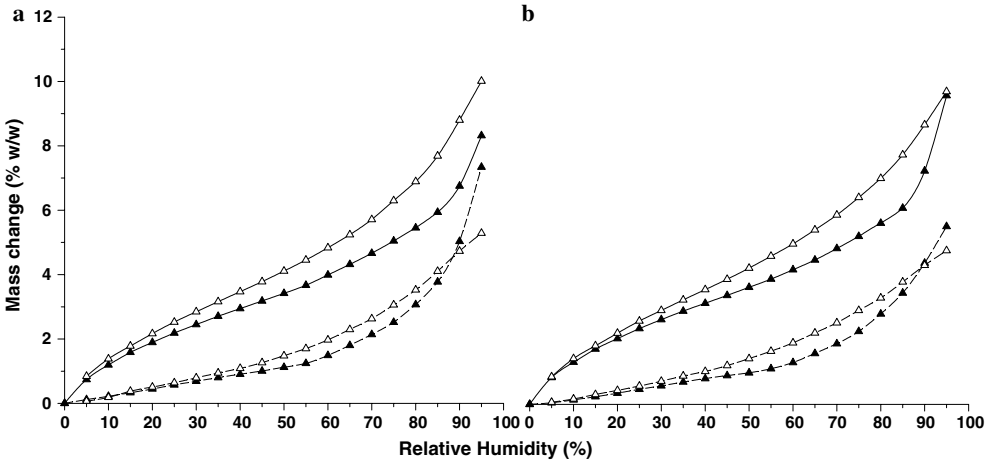

Fig. 4. Fast (solid lines) and slow (dashed lines) components of sorption (full symbols) and desorption (empty symbols) process for SMCC (a) and MCC (b), according to the PEK model.

In other words, the slow process of moisture sorption clearly predominates only for the case of SMCC at high relative humidity. This again may be attributed to the hydrolysis of SiO_2 and formation of silanol groups operating as new hydrophilic sites on the surface of SMCC. Since the formation of silanol groups demands energy, it probably proceeds slowly and is modelled by the "slow" component of the PEK model. This can also be shown by the reconstructed fast and slow sorption–desorption component isotherms, Figs. 4(a) and (b).

The plots in Figs. 4(a) and (b) are obtained by adding the amount of water sorbed (or desorbed) at each RH level to that already sorbed (or desorbed) at previous RH levels and therefore represent the cumulative sorption–desorption by the two processes separately. They show that the fast sorption component (solid lines and full symbols) retains the type II shape of the experimental sorption isotherm, while the slow sorption components (dashed lines and full symbols) have a nearly type III shape (Flory-Huggins isotherm). This further supports the interpretation of the slow sorption as a non-specific process. To test this assumption, using the determined values of crystallinity index (0.83 ± 0.05 and 0.84 ± 0.05 for SMCC and MCC, respectively) and calculating the number of water molecules per anhydroglucose unit sorbed by the fast process, we obtain values of 4.2–4.4. Taking into account that the method applied in this study tends to overestimate crystallinity [33], these values are reasonably close to the experimental bound water value of 3.4, reported by Hatakeyama [14].

From Figs. 4(a) and (b) it is also seen that hysteresis is higher in the fast components than that in the slow. This is in agreement with the view that hysteresis is caused by structural changes due to the disruption of the hydrogen bonding network of the polymer by the interaction with water molecules, and to a lesser extent when water molecules are incorporated into the polymer matrix in a mixing-like manner. Furthermore, for both polymers, the slow components of processes in Figs. 4(a) and (b) show that more water is sorbed than desorbed by the slow processes. This "extra water" should be interpreted as "water that is stored at newly generated sites" according to Kohler et al. [15], and for MCC, the amount of this "extra" water is small (about 0.8%), but in the case of SMCC it is about 2%. Therefore, for MCC the fast component isotherms form an almost closed loop, while for SMCC obviously much more "extra" water needs to be added to the fast sorption component in order to close the loop. This means that primarily for SMCC and secondarily for MCC, some water that is sorbed by the slow process is actually desorbed by the fast process.

The explanation of "extra" water should be related to structural changes, and particularly for MCC, to conformational changes of cellulose chains that expose previously inaccessible high affinity (fast) sorption sites [9]. For SMCC, the high amount of "extra" water cannot be explained solely by the conformational changes of cellulose. A possible explanation may be that adsorption of water on SiO_2 particles initially takes place by diffusion, not involving specific interactions (slow process), but following the formation of silanol groups, water is associated by hydrogen bonds. Therefore, desorption of water from silanol groups takes place by the fast process, indicative of specific interactions between water and solid. In other words, SiO_2 particles may act as a water sink at high relative humidity, preventing more water to interact with cellulose chains and thus protecting its structure from changes that may be irreversible. This behaviour might be the key to SMCC's improved functionality as wet granulation excipient [34].

4. Conclusions

On the basis of the kinetic models, in general, the differences in the moisture sorption and desorption properties of MCC and SMCC can be elucidated. Particularly the PEK model shows that hysteresis is related primarily to the fast sorption process, which corresponds to bound water, and

secondarily to the slow process, which corresponds to sorption of free water and that SMCC acquires more water than MCC at RH higher than 50% by the slow (secondary) sorption process. A possible mechanism for this process may be the hydrolysis of SiO_2 particles and formation of silanol groups that act as a water reservoir, preventing the accumulation of more water in the polymer matrix and thus protecting the structure of SMCC from undergoing irreversible structural changes that would impair its performance as an excipient.

References

[1] G.K. Bolhuis, Z.T. Chowan, Materials for direct compaction, in: G. Alderborn, C. Nyström (Eds.), Pharmaceutical Powder Compaction Technology, Dekker, New York, 1996, pp. 419–501.

[2] J.N. Staniforth, M. Chatrath, Towards a new class of high functionality tablet binders, I: Quasi-hornification of microcrystalline cellulose and loss of functionality, Pharm. Res. 13 (1996) S208.

[3] F. Doelker, Comparative compaction properties of various microcrystalline cellulose and generic products, Drug Dev. Ind. Pharm. 19 (1993) 2399–2471.

[4] B.E. Sherwood, J. Becker, A new class of high functionality excipients: silicified microcrystalline cellulose, Pharm. Technol. 22 (1998) 183–194.

[5] M.J. Tobyn, G.P. McCarthy, J.N. Staniforth, S. Edge, Physicochemical comparison between microcrystalline cellulose and silicified microcrystalline cellulose, Int. J. Pharm. 169 (1998) 183–194.

[6] G. Buckton, E. Yonemochi, W.L. Yoon, A.C. Moffat, Water sorption and near IR spectroscopy to study the differences between microcrystalline cellulose and silicified microcrystalline cellulose before and after wet granulation, Int. J. Pharm. 181 (1999) 41–47.

[7] K. Kachrimanis, I. Nikolakakis, S. Malamataris, Tensile strength and disintegration of tableted silicified microcrystalline cellulose: influences of interparticle bonding, J. Pharm. Sci. 92 (2003) 1489–1501.

[8] A. Mihranyan, A. Llagostera, R. Karmhag, M. Strømme, R. Ek, Moisture sorption by cellulose powders of varying crystallinity, Int. J. Pharm. 269 (2004) 433–442.

[9] S. Airaksinen, M. Karjalainen, A. Shevchenko, S. Westermarck, E. Leppänen, J. Rantanen, J. Yliruusi, Role of water in the physical stability of solid dosage formulations, J. Pharm. Sci. 94 (2005) 2147–2165.

[10] S.H. Zeronian, M.L. Coole, K.W. Alger, J.M. Chandler, Studies on the water sorption isotherms of celluloses and their use for determining cellulose crystallinities, J. Appl. Polym. Sci. Appl. Polym. Symp. 37 (1983) 1053–1069.

[11] G. Zografi, M.J. Kontny, A.Y. Yang, G.S. Brenner, Surface area and water vapour sorption of microcrystalline cellulose, Int. J. Pharm. 18 (1984) 99–116.

[12] F. Khan, N. Pilpel, An investigation of moisture sorption in microcrystalline cellulose using sorption isotherms and dielectric response, Powder Technol. 50 (1987) 237–241.

[13] C. Fringant, J. Desbrières, M. Milas, M. Rinaudo, C. Joly, M. Escoudes, Characterization of sorbed water molecules on neutral and ionic polysaccharides, Int. J. Biol. Macromol. 18 (1996) 281–286.

[14] H. Hatakeyama, T. Hatakeyama, Interaction between water and hydrophilic polymers, Thermochim. Acta 308 (1998) 3–22.

[15] R. Kohler, R. Dueck, B. Ausperger, R. Alex, A numeric model for the kinetics of water vapour sorption on cellulosic reinforcement fibers, Composite Interfaces 10 (2003) 255–276.

[16] L. Segal, J. Creely, A. Martin Jr., C. Conrad, An empirical method for estimating the degree of crystallinity of native cellulose using the X-ray diffractometer, Text. Res. J. 29 (1959) 786–794.

[17] S. Okubayashi, U. Griesser, T. Bechtold, A kinetic study of moisture sorption and desorption on lyocell fibers, Carbohyd. Polym. 58 (2004) 293–299.

[18] J. Adolphs, M.J. Setzer, A model to describe adsorption isotherms, J. Colloid Interface Sci. 180 (1996) 70–76.

[19] J. Adolphs, M.J. Setzer, Energetic classification of adsorption isotherms, J. Colloid Interface Sci. 184 (1996) 443–448.

[20] J. Adolphs, M.J. Setzer, Description of gas adsorption isotherms on porous and dispersed systems with the excess surface work model, J. Colloid Interface Sci. 207 (1998) 349–354.

[21] C. Van der Berg, Vapour sorption equilibria and other water–starch interactions: a physicochemical approach, Ph.D. Thesis, Agricultural University of Wageningen, Wageningen, 1981, pp. 106–110.

[22] E.O. Timmermann, Multilayer sorption parameters: BET or GAB values? Colloid Surf. A: Physicochem. Eng. Aspects 220 (2003) 235–260.

[23] J. Young, G. Nelson, Theory of hysteresis between sorption and desorption isotherms in biological materials, Trans. Am. Soc. Agric. Eng. 10 (1967) 260–263.

[24] J. Young, G. Nelson, Research of hysteresis between sorption and desorption isotherms of wheat, Trans. Am. Soc. Agric. Eng. 10 (1967) 756–761.

[25] A. Nokhodchi, J. Ford, M. Rubinstein, Studies on the interaction between water and (hydroxypropyl)methylcellulose, J. Pharm. Sci. 86 (1997) 608–615.

[26] C.L. Lomauro, A.S. Bakshi, T.P. Labuza, Evaluation of food moisture sorption isotherms equation. Part I: Fruit, Lebensm. Wiss. U Technol. 18 (1985) 111–117.

[27] W.E. Morton, J.W. Hearle, Physical properties of textile fibres, The Textile Institute, UK, 1997.

[28] K. Matsumoto, Y. Nakai, T. Oguchi, K.Y. Yamamoto, Effect of pore size on the gaseous adsorption of ethenzamide on porous crystalline cellulose and the physicochemical stability of ethenzamide after storage, Chem. Pharm. Bull. 46 (1998) 314–318.

[29] V. Murashov, Ab initio cluster calculations of silica adsorption sites, J. Mol. Struct. 650 (2003) 141–157.

[30] T. Bakos, S.N. Rashkeev, S.T. Pantelides, Reactions and diffusion of water and oxygen molecules in amorphous SiO_2, Phys. Rev. Lett. 88 (2002) 1–4.

[31] P. Ravikovitch, S. Domhnaill, A. Neimark, F. Schüth, K. Unger, Capillary hysteresis in nanopores: theoretical and experimental studies of nitrogen adsorption on MCM-41, Langmuir 11 (1995) 4765–4772.

[32] F. Rouquerol, J. Rouquerol, K. Sing, Adsorption by Powders and Porous Solids. Principles, Methodology and Applications, Academic Press, San Diego, CA, 1999.

[33] A. Thygesen, J. Oddershede, H. Lilholt, A. Thomsen, K. Stahl, On the determination of crystallinity and cellulose content in plant fibres, Cellulose 12 (2005) 563–576.

[34] B. Sherwood, J. Becker, A new class of high functionality excipients: silicified microcrystalline cellulose, Pharm. Technol. 22 (1998) 183–194.